(12) **UK Patent Application** (19) **GB** (11) **2 360 186** (13) **A**

(21) Application No 0005225.8

(22) Date of Filing 03.03.2000

(71) Applicant(s)
   Teraprobe Limited
   (Incorporated in the United Kingdom)
   Five Chancery Lane, London, EC4A 1BU,
   United Kingdom

(72) Inventor(s)
   Craig Michael Ciesla
   Donald Dominic Arnone
   Bryan Edward Cole

(74) Agent and/or Address for Service
   Marks & Clerk
   57-60 Lincoln's Inn Fields, LONDON, WC2A 3LS,
   United Kingdom

(51) INT CL[7]
   G01N 21/49

(52) UK CL (Edition S)
   H5R RAD RAT RTQ

(56) Documents Cited
   EP 0864857 A1   EP 0828162 A2   EP 0828143 A1
   US 5710430 A

(58) Field of Search
   UK CL (Edition R) G1A AAMA AAMX , H5R RAD RAT
   RTQ
   INT CL[7] A61B 5/00 6/14 , G01N 21/35 21/47 21/49
   21/84
   Online:WPI, JAPIO, EPODOC

(54) Abstract Title
   Investigating or imaging a sample using reflected terahertz pulses

(57)   A range of technique for investigating a sample such as obtaining images and/or spectral information are described. The techniques include a method for deriving structural information about a sample as a continuous function of the depth below the surface of the sample, a method for evaluating a part of the structure of a sample located between two interfaces within the sample, and a contrast enhancing method and apparatus which has a quick image acquisition time.
   The technique comprises irradiating the sample with pulses of radiation from millimetre wavelength through to the far infra-red (i.e. 25GHz to 100THz) which is often referred to as Terahertz radiation. The reflected and/or transmitted pulses may be analysed as a function of time.

Fig. 1

At least one drawing originally filed was informal and the print reproduced here is taken from a later filed formal copy.

The print reflects an assignment of the application under the provisions of Section 30 of the Patents Act 1977.
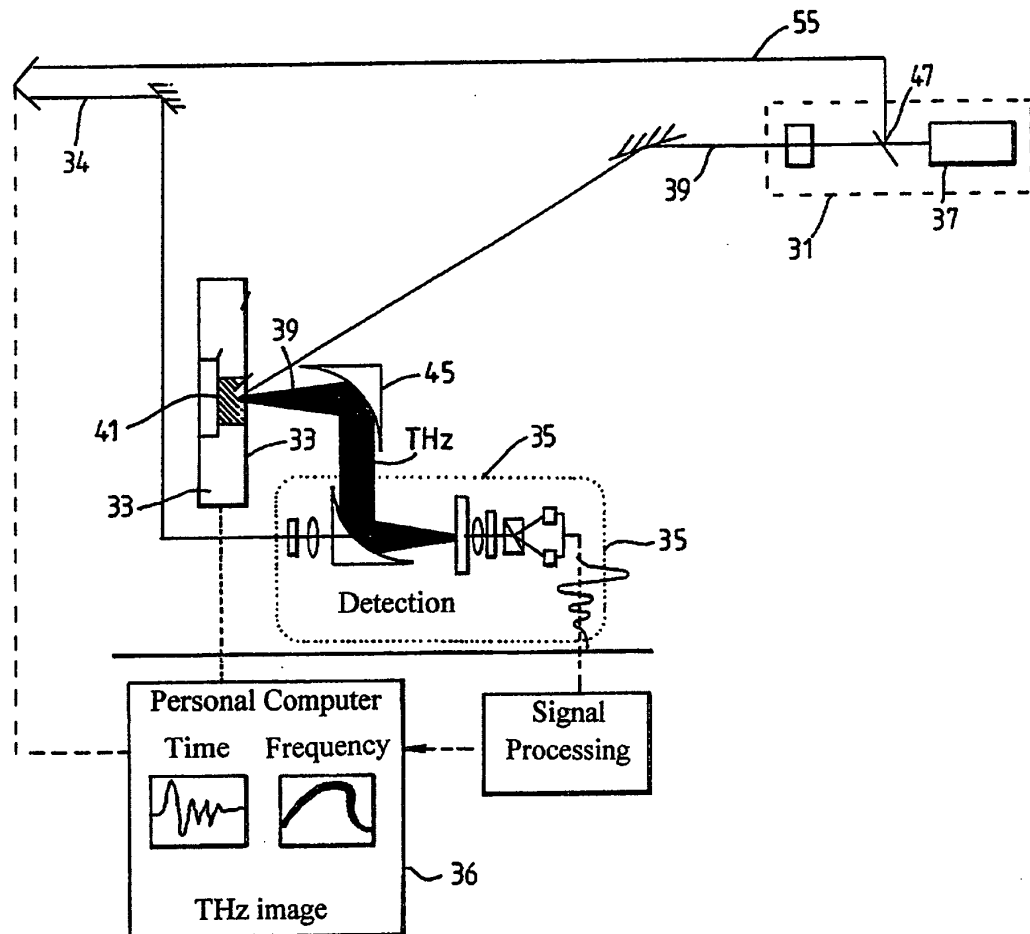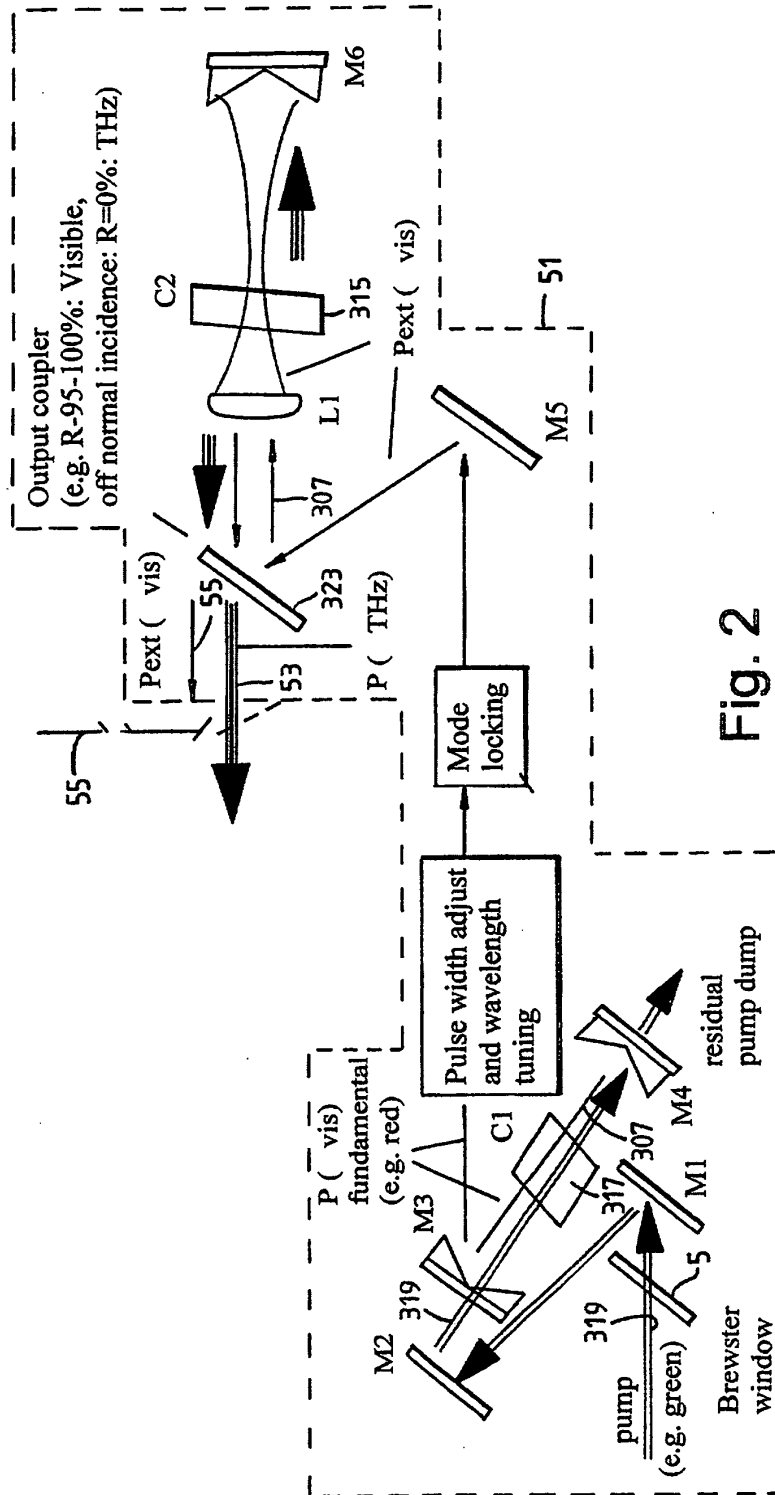
GB 2 360 186 A
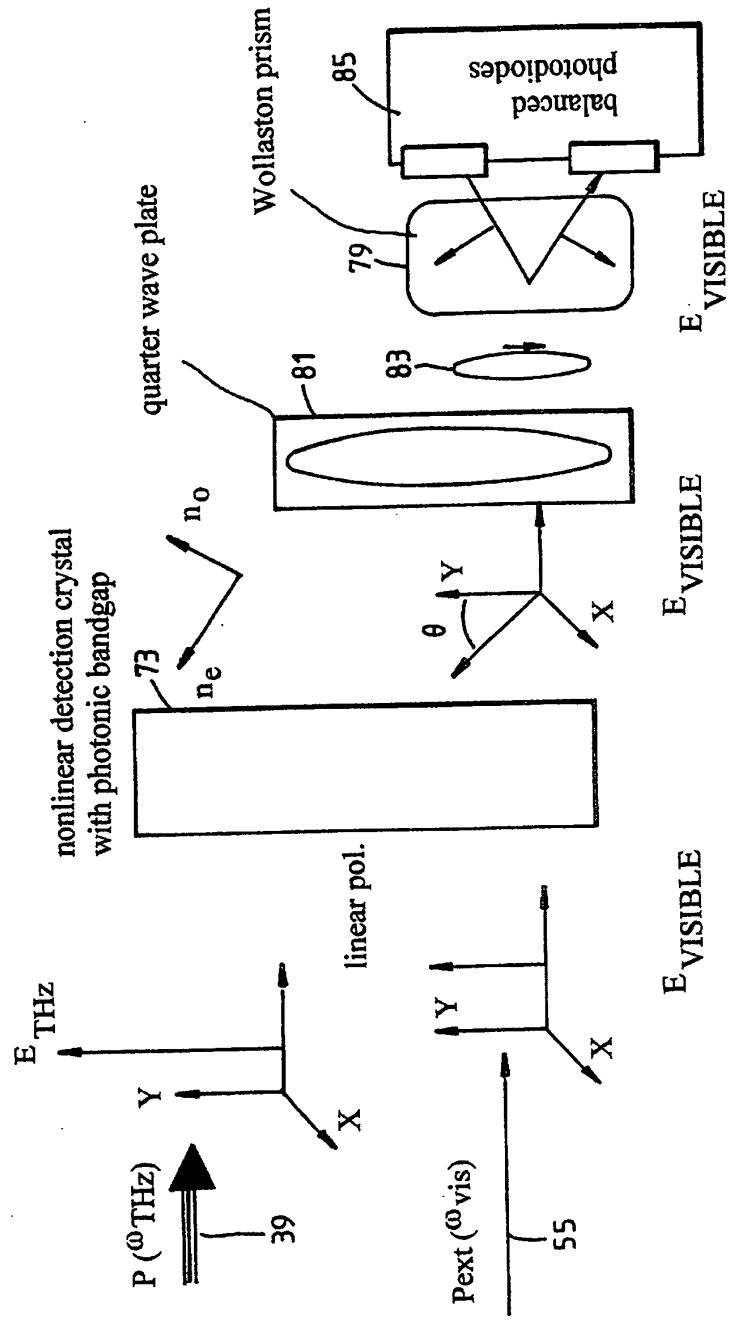
Fig. 1

Fig. 2

Fig. 3

Fig. 4

ω_1

ω_2

97a

97b

E - field

Lens - hemispherical or
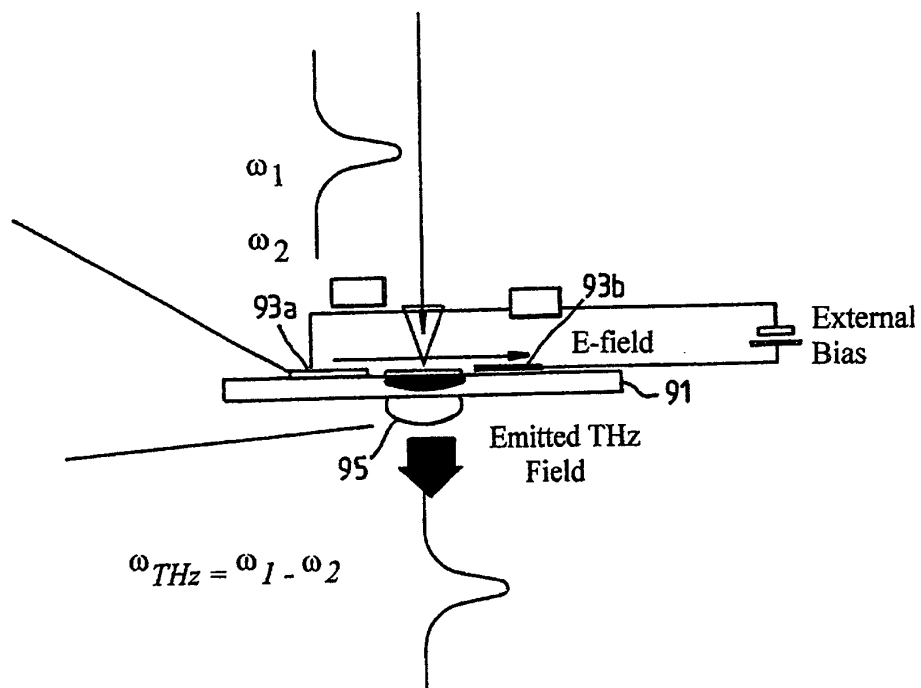other design
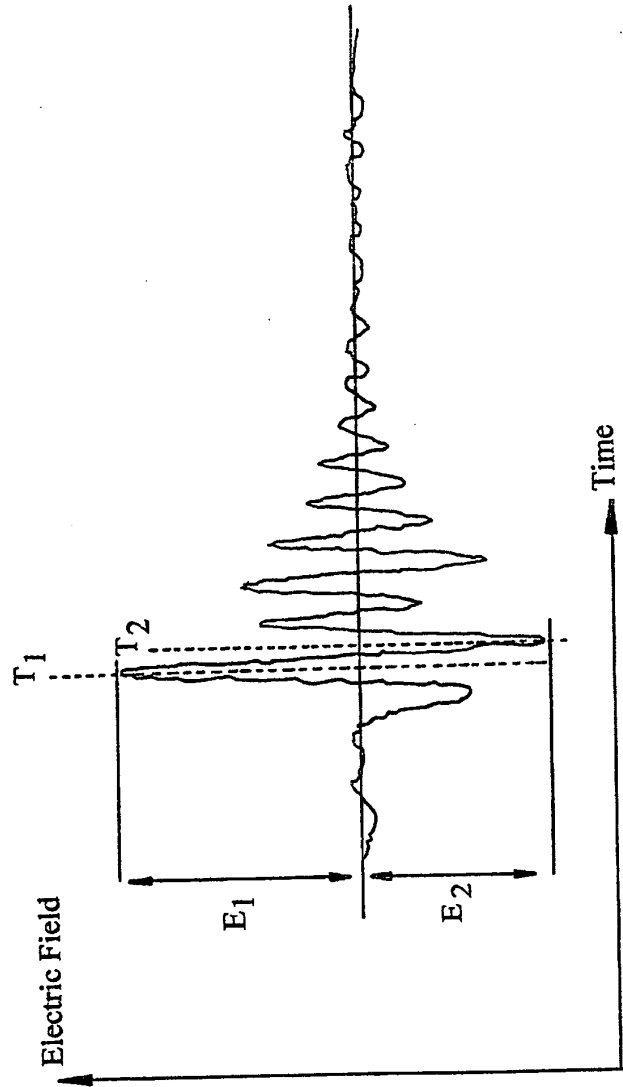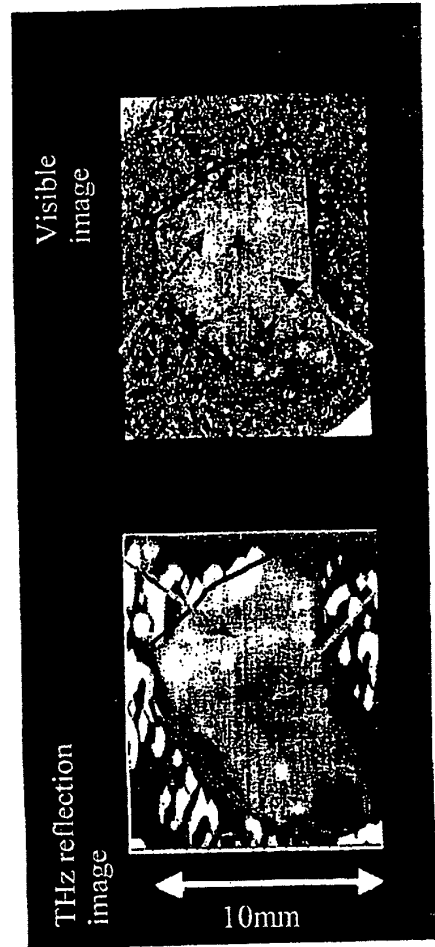
96

98

Incident THz
Field

$\omega_{THz} = \omega_1 - \omega_2$

Fig. 5

Fig. 6

Fig. 7(a)   Fig. 7(b)

Fig. 8a

Fig. 8b

Fig. 9(a)

Fig. 9(b)

Fig. 9(c)

Fig. 9(d)

Fig. 9(e)
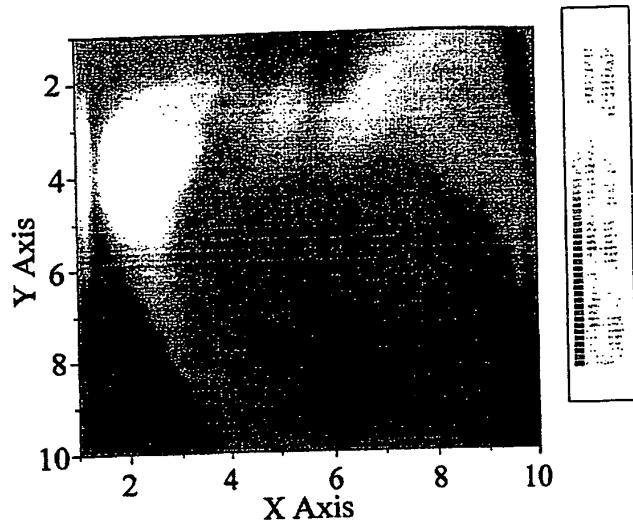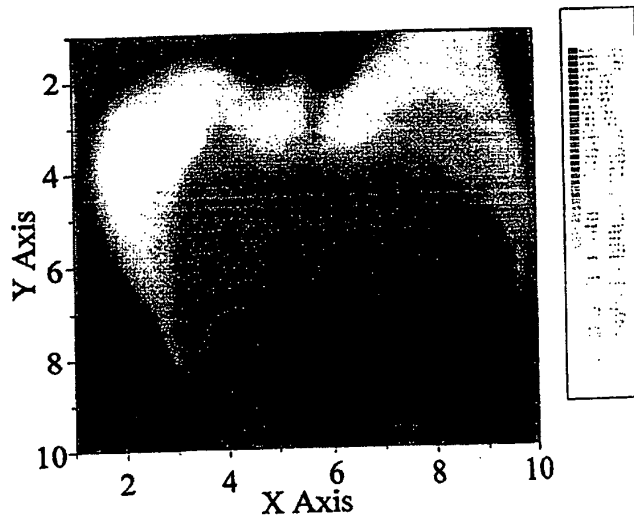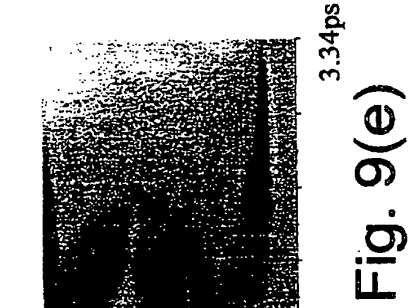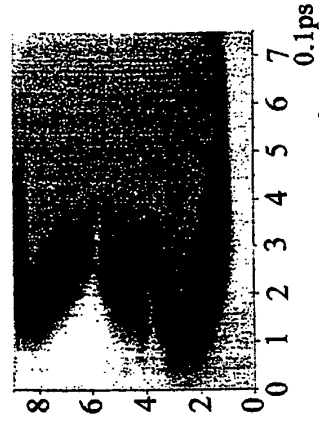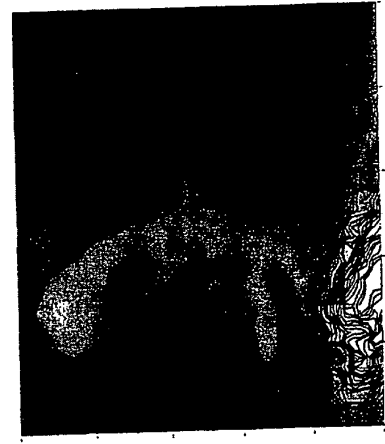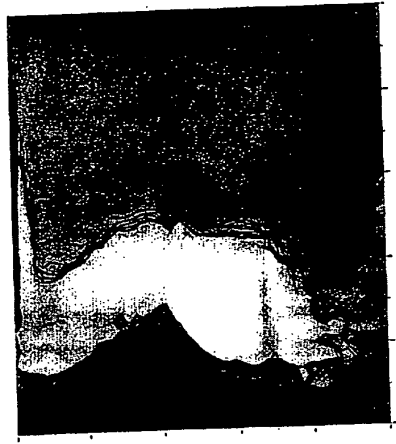
Fig. 10(c)

Fig. 10(d)

Fig. 10(a)

Fig. 10(b)
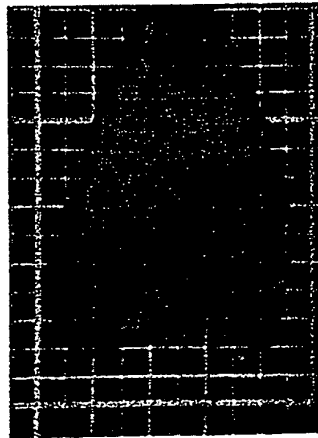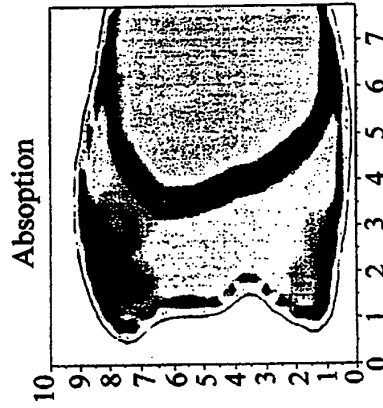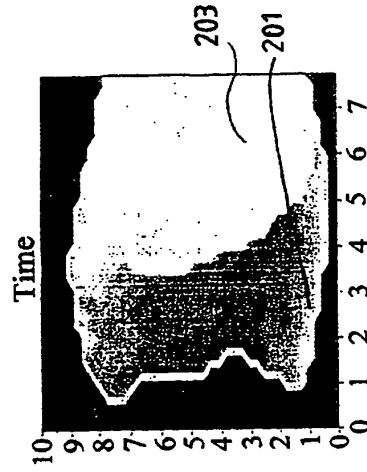
Fig. 11(a)
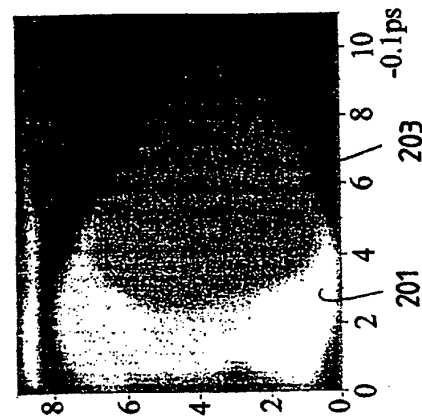
Fig. 11(b)

Fig. 11(c)

Fig. 11(d)

Fig. 11(e)

Fig. 11(f)

Fig. 12(a)

Absorption

Fig. 12(b)

Time Slice 99

Fig. 12(c)

Max Peak
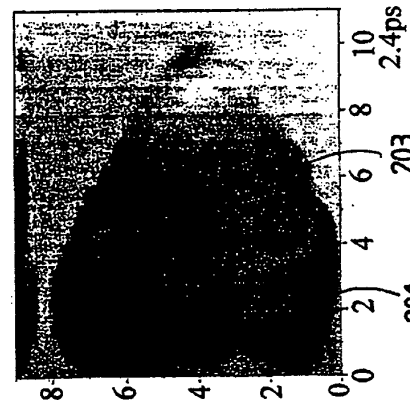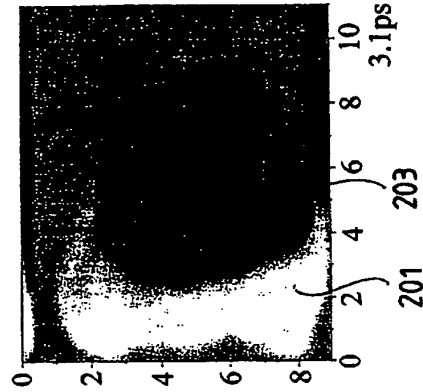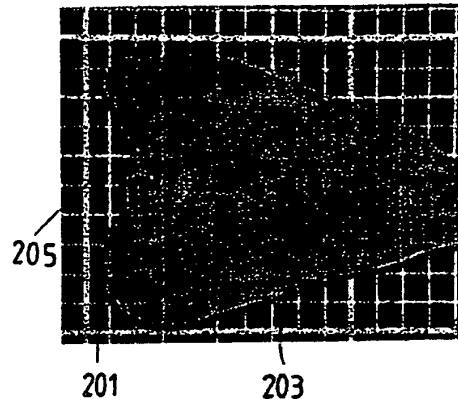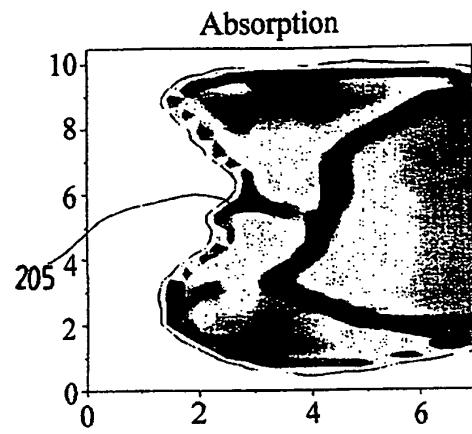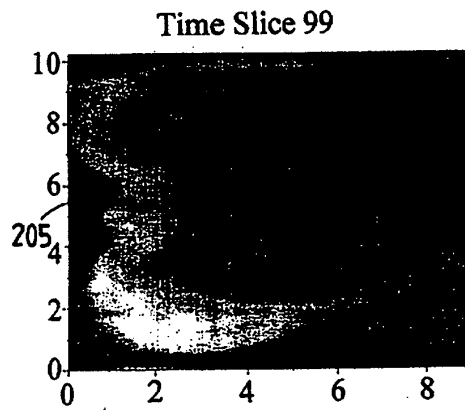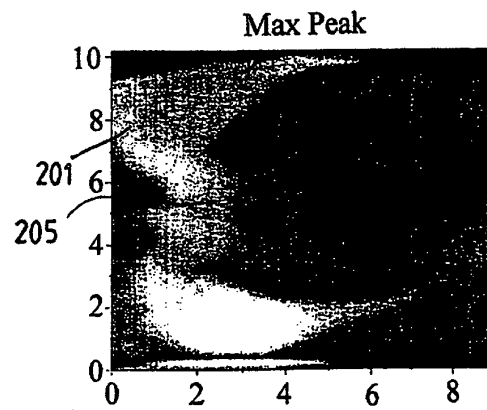
Fig. 12(d)

Detection of Caries - Reflection Imaging

Fig. 13(a)

Fig. 13(b)

Example **Reflection at each interface**

#1 : Enamel

#2 : Enamel-Dentine

#3 : Dentine-Pulp Cavity

THz Pulse Laboratory
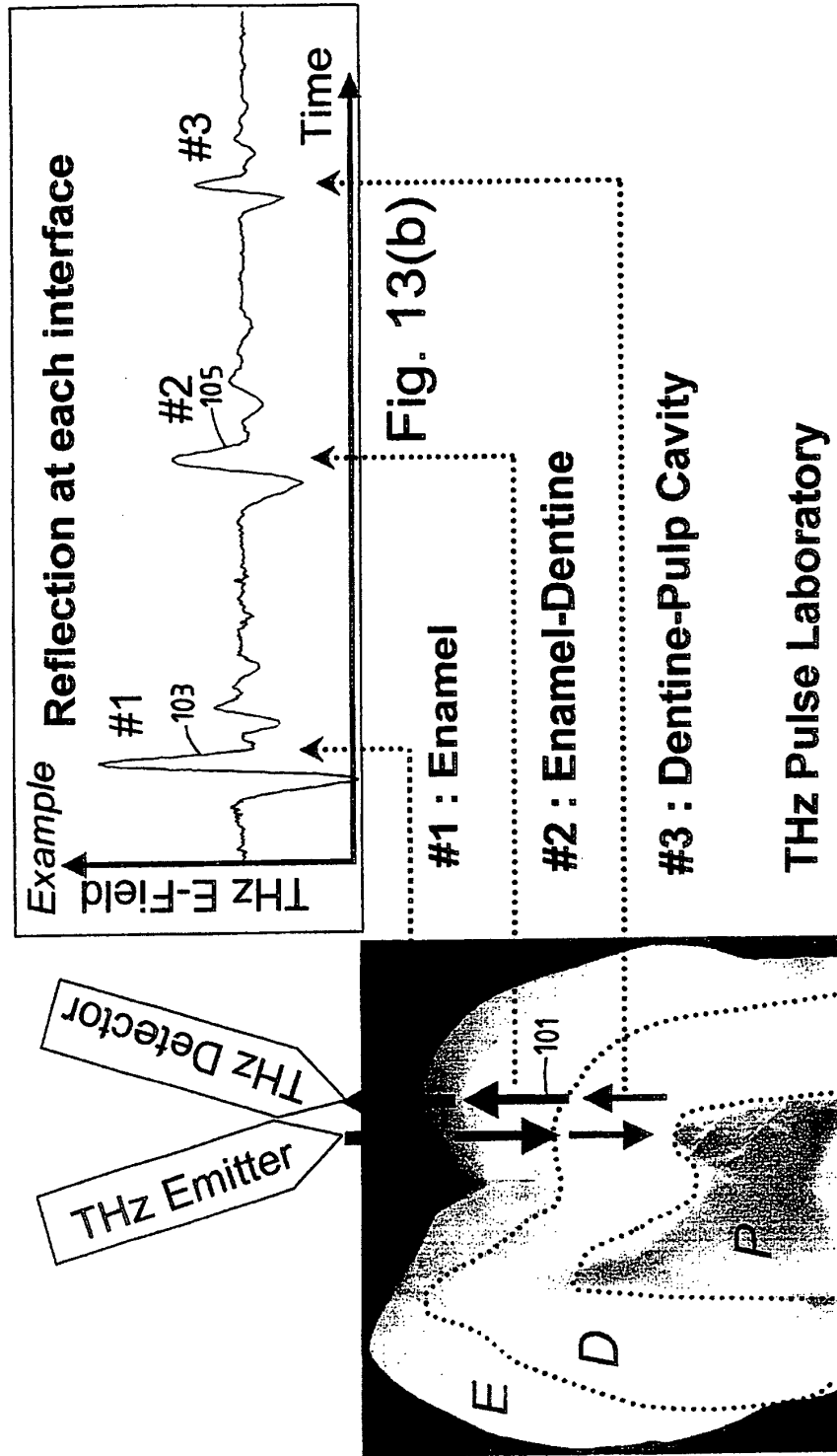
Detection of Caries - Reflection Imaging

- Ratio of first two peaks to measure absorption of enamel layer – identify caries by enhanced absorption

- Time shift gives the layer thickness - 3D Imaging
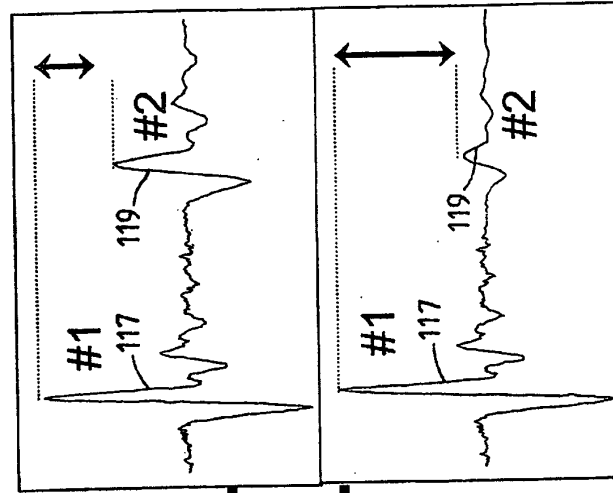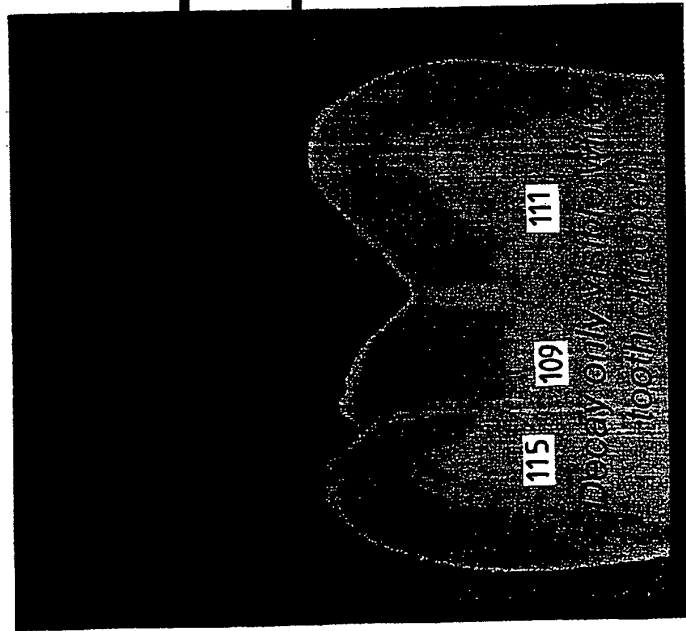
Low absorption
HEALTHY

Fig. 14(b)

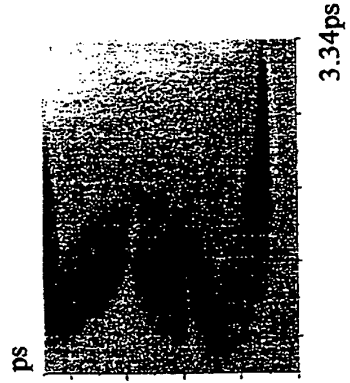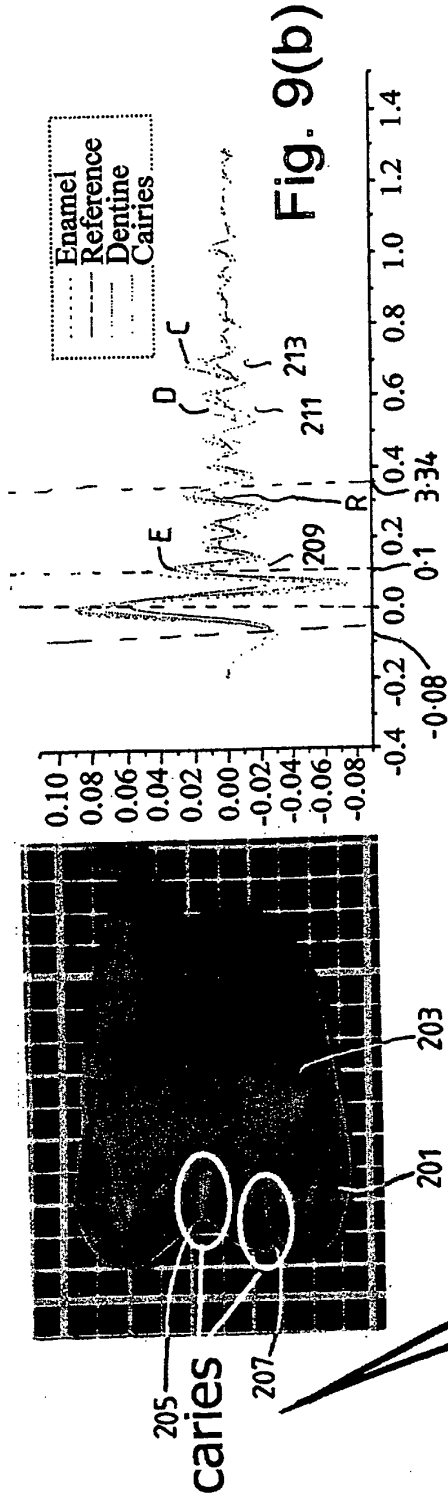High absorption
CARIES

Fig. 14(c)

Fig. 14(a)

THz Pulse Laboratory
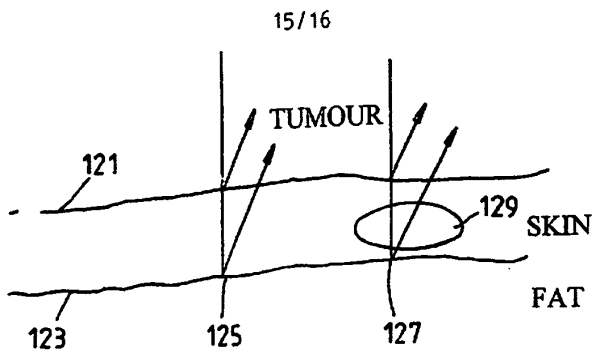
Fig. 15(a)
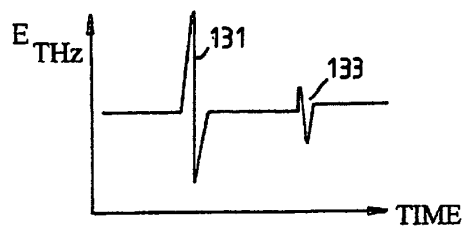
Fig. 15(b)
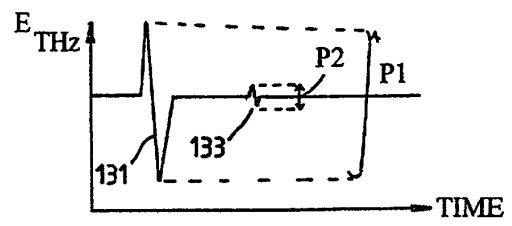
Fig. 15(c)
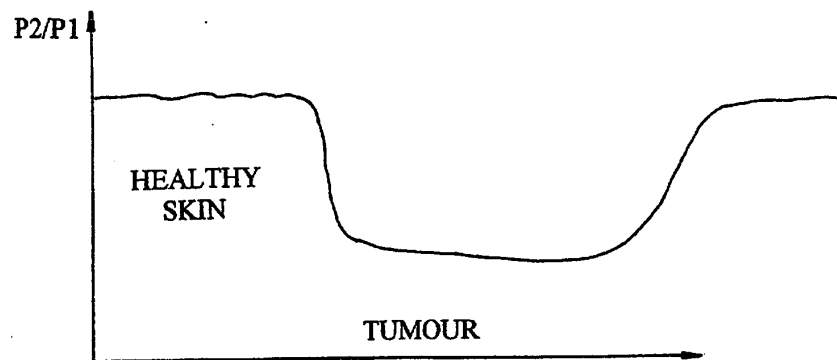
Fig. 15(d)
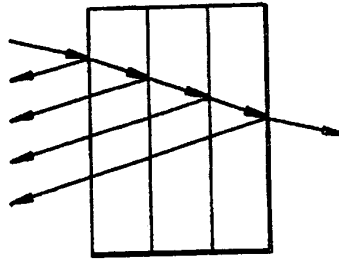
Fig. 16

Apparatus and Method for Investigating a Sample

The present invention is concerned with the field of investigating and imaging samples primarily using radiation in the frequency range from 25GHz to 100THz. This frequency range extends from the mid infrared range up to, and including the lower end of the microwave range. This range of frequencies encompasses the Terahertz (THz) range and is generally referred to as THz radiation.

Such radiation is non-ionising and, as a result, it is particularly of use in medical applications. In any type of medical imaging, radiation is generally reflected from or transmitted through the patient. Radiation in the above frequency range is generally quite heavily absorbed in structures having a high water content. Therefore, reflection measurements are believed to be of particular use in such investigations.

Reflection measurements in non-lossy materials have been previously demonstrated in EP 0 864 857. This document explains how to perform simple analysis using reflection measurements on non-lossy materials which have sharp discontinuities in their refractive index. The position of the dielectric interfaces within a floppy disc is used to demonstrate the technique.

However, medical samples in general are particularly lossy media, in other words, Terahertz radiation is strongly absorbed in such structures. Also, there is a need to be able to determine the structure of sample which does not have sharp discontinuities in its refractive index.

The present invention seeks to address the above problems, and in a first aspect, provides a method of imaging a sample, the method comprising the steps of:

irradiating a surface of a sample with pulse of electromagnetic radiation. said
pulse having a plurality of frequencies in the range from 25 GHz to 100 THz;

detecting said radiation reflected from the sample and deriving information
about the structure of the sample as a function of depth from the surface of the sample

The above method is ideally intended for use with biological samples. Also, the above
method derives information as a continuous function of the depth from the surface of
the sample. Preferably either the refractive index or the absorption coefficient is derived
as a function of depth from the surface of the sample. The structural information can be
derived as a continuous analytical function of the measured reflected radiation.

Preferably, the method further comprises the step of obtaining a reference signal. The
said reference signal is preferably a signal taken without the presence of the sample and
is preferably obtained by reflecting the radiation off a mirror which has substantially
perfectly reflecting.

The above method uses reflections from the sample in order to obtain information about
the continuously changing absorption coefficient, refractive index and other structural
parameters of the sample. The technique does not rely on the present of sharp
discontinuities within the sample to derive information about specific regions of the
sample, because the method provides an analytical technique for deriving a continuously
changing parameter as a function of depth.

It is possible to perform this analysis using the above method as the wavevector of each
frequency component of the THz pulse is dominated by the absorption coefficient as
opposed to the refractive index (which is the case for lossless media). Preferably the
frequency range from 50GHz to 80THz is used, more preferably from 100GHz to
50THz.

In a second aspect, the present invention provides an apparatus for investigating a
sample, the apparatus comprising:

means for irradiating a surface of a sample with a pulse of electromagnetic radiation, said pulse having a plurality of frequencies in the range from 25 GHz to 100 THz;

means for detecting said radiation reflected from the sample and deriving structural information about the sample as a function of depth from the surface of the sample.

Of course, it is possible to study samples which have sharp discontinuities in the refractive index using the above method. In both lossless and lossy media, the signal due to reflection from a discontinuity in the refractive index such as an internal dielectric interface or an external surface of the sample can be easily detected. Such a signal usually manifests itself in terms of a large peak in the reflected radiation which can be easily detected.

This reflection data can be used to determine the position of interfaces within the same. However, it can also be used to obtain data concerning the absorption of the sample between the two interfaces. Comparing the signals from different interfaces in different parts of the sample, is particularly of use in studying samples where there is some variation in the absorption of the latter between the two interfaces.

Therefore, in a third aspect, the present invention provides a method for studying a sample, the method comprising the steps of:

irradiating a first part and a second part of a surface of the sample with electromagnetic radiation having a frequency in the range from 25 GHz to 100THz, the first interface being located closer to the surface than the second interface;

detecting the signal due to reflection of the radiation from the first and second interfaces of the two parts of the sample; and

comparing the peak height of the signal from the second interface with that from the first interface to produce a connected second interface signal and comparing the connected second interface signals.

The step of comparing the signal from the first interface with that of the second could comprise the step of dividing the peak height of the signal from the second interface with that from the first or subtracting the signals. Alternatively, the method could comprise the step of comparing the two signals from the two different parts of the sample with respect to the peak height.

Comparing the peak heights of the signal from the first and second interfaces allows any variations in detected radiation due to differences in the sample position and differences in the sample which are not between the first and second interfaces to be taken into account..

The above method is particularly of use when looking for an abnormality in a sample. For example, looking for a skin tumour. In such a sample, there will be a reflection from an interface above the tumour such as the external surface of the skin, there will also be a reflection from an interface below the skin, for example, the skin/fat interface. A tumour has been shown to absorb THz quite strongly. Therefore, the signal from the second interface will be weaker in a tumourous region than in a non tumourous region.

Hence, one of the parts of the sample is preferably a healthy part which is used as a reference.

Further, by scanning the THz beam across the skin while looking at the relative height of the signal from the second interface with respect to the first, it is possible to build up a picture of the extent of the tumour.

The above method is not only limited to looking for tumours. It has been shown that areas of teeth which have been subjected to dental caries are also more strongly absorbing than healthy areas of the teeth. Therefore, there will be a marked change in the signal from the second interface from the healthy region of the teeth to the carious region of the teeth.

The above method may comprise the step of looking at many different parts of the sample, and generating a plot of the corrected second peak against the position on the sample. An image of the sample could also be built up by plotting the corrected second peak against the position on the sample.

To build up a 2D image, an area of the sample is subdivided into pixels and the reflected radiation form each of the pixels is detected.

The radiation used can be pulsed radiation which comprises a plurality of frequencies or even continuous wave radiation which has substantially a single frequency.

In a fourth aspect, the present invention provides an apparatus for generating an image of a sample, the apparatus comprising:

means for irradiating a sample with a pulse of electromagnetic radiation, said pulse having a plurality of frequencies in the range from 25 GHz to 100 THz;

means for detecting the amplitude of the radiation reflected from or transmitted by the sample; and

means for generating an image of sample using the amplitude of the radiation detected at a single point in time.

When studying a sample, it is usually desirable to generate and image of the sample. Typically, images of the sample have been generated by plotting the maxima or minima of the detected Terahertz radiation. However, it has been found that a better contrast can be obtained by looking at the THz electric field for a particular time delay.

Therefore, in a fifth aspect, the present invention provides a method of imaging a sample, the method comprising the steps of:

irradiating a sample with a pulse of electromagnetic radiation, said pulse having a plurality of frequencies in the range from 25 GHz to 100 THz;

detecting the amplitude of the radiation; and

generating an image of sample using the amplitude of the detected radiation at a particular point in time.

In order to generate an image, it is necessary to measure the THz signal from a number of different parts of the sample. Typically, the area of the sample which is to be imaged will be subdivided into a two-dimensional array of pixels and the radiation will be detected from each of the pixels. In order to detect radiation from each of the pixels, the sample may be moved relative to the beam of radiation or the beam may be moved relative to the sample, or both. Alternatively, the whole area of the sample could be irradiated and the radiation transmitted through or detected form the area of the sample could be detected by a CCD camera or the like.

The Terahertz pulse which is used to irradiate the sample will spread out due to its passage through the sample. As a result, different parts of the pulse will be detected at different times. The leading edge of the pulse of a particular features of the pulse, can be thought of as arriving at the detector at a time $t=0$, then the other parts of the pulse will arrive at the detector with a delay time "t".

The method of the fifth aspect of the present invention generates an image using a specific 't'.

The radiation can be detected at a specific time 't', this is advantageous as it does not require detecting radiation for every 't' and hence the acquisition time of the image is substantially improved.

Alternatively, it may be desirable to detect the radiation for a range of 't' and then select a particular "t" in order to generate the image. This allows an image to be scannable using "t" as the scanning variable. Thus, someone using the method could scan the image for various "t" until the image with the best contrast was obtained.

This method could be used for either or both of transmitted data or reflected data.

In a sixth aspect, the present invention provides an apparatus for imaging a sample comprising:

means for irradiating a sample with a pulse of electromagnetic radiation, said pulse having a plurality of frequencies in the range from 25 GHz to 100 THz;

means for detecting the amplitude of the radiation reflected from or transmitted by the sample; and

means for generating an image of sample using the amplitude of the radiation detected at a single point in time.

The apparatus preferably further comprising means for displaying a plurality of images generated from different time points. More preferably, the apparatus comprises optimising means for optimising the image using the variable parameter of the delay time.

The present invention will now be described with reference to following preferred non-limiting embodiments:

Figure 1 shows a schematic imaging system in accordance with an embodiment of the present invention;

Figure 2 shows an example of a generation section for use with the imaging system of Figure 1;

Figure 3 shows an example of a detection section for use with the imaging system of Figure 1;

Figure 4 shows a further example of a generator for use with the imaging system of Figure 1;

Figure 5 shows a further example of a detector for use with the imaging system of Figure 1;

Figure 6 shows a schematic trace of a pulse detected by the imaging system of Figure 1;

Figure 7 shows an image of a skin carcinoma produced in accordance with an embodiment of the present invention;

Figures 8a and 8b shows two images of a tooth produced using a method in accordance with an embodiment of the present invention;

Figure 9a shows a visible image of a slice through a tooth, figure 9b shows a typical THz time domain trace for a tooth, figures 9c, d and e show time slice images for the tooth at delayed times -0.08ps, 0.1ps and 3.34ps;

Figure 10a to 10a show four images of time slices through the tooth shown in Figure 9A;

Figure 11a shows a visible image of a tooth, Figure 11b shows an absorption image of the tooth of Figure 11a, Figure 11c shows a time of flight image of the tooth of Figure 11a, Figures 11d to 11f show time slices of the tooth of Figure 11a for times -0.1ps, 2.4ps and 3.1ps respectively;

Figure 12a shows a visible image of a tooth, Figure 12b shows the absorption image of that tooth, Figure 12c shows a time slice through that tooth and Figure 12d shows an image of the tooth plotting the time of the maximum peak of the electric field;

Figure 13 shows a visible image of a tooth and a THz signal from the tooth;

Figure 14 shows a visible image of a tooth and two THz traces of diseased and healthy parts of the tooth;

Figure 15 is a schematic of skin and shows a schematic signal from the skin; and

Figure 16 shows a schematic layer structure of a sample which can be investigated using a method in accordance with an embodiment of the present invention;

Figure 1 shows a basic THz imaging system. The system can be simplified into three main sections, a generator 31, an imaging section 33 and a detection section 35. THz radiation is generated in the generating section 31 by using a THz emitter which is supplied by a visible pulsed laser 37.

A THz beam 39 is emitted from generation section 31 and is directed onto sample 41 of the imaging section 33. The THz beam 39 is then reflected from sample 41 and directed via further optics 45 into the detection section 35. The THz beam which is reflected from the sample 41 is beam 39.

The detection section reads the information carried in the detected THz signal via a visible light signal and AC Pockels effect. The visible light can be obtained from laser 37 via beam splitter 47. Laser 37 is a Ti : Sapphire laser which typically produces wavelengths in the range of 900nm to 350nm, with a pulse width of 50fs and a repetition rate of 82 MHz.

Beam splitter 47 splits the beam into a reference beam 55 and a beam for THz generation. A time delay is added to the reference beam 55 via time delay line 34. Varying the time delay via the time delay line allows the phase of the reference beam to be varied with respect to that of the THz beam 39. This is used in detecting the THz beam in detection system 35. The system (e.g. the control of the sample 41 movement, the time delay 34 and the detected signal processing) is controlled by computer 36. Details of the AC Pockels effect will be described with reference to Figure 3.

Figure 2 shows a generator which can be used with the imaging system of Figure 1. Here, for simplicity, details of the detection part of the system will be omitted. These will be described with reference to Figure 3.

Figure 2 shows a THz generator using a frequency conversion member which may be a crystal which non-linear properties of the like such as ZnTe. The radiation used to generate the THz radiation via frequency conversion member 315. Radiation is supplied to frequency conversion member 315 from Ti:Sapphire crystal 317. Ti:Sapphire crystal 317 emits a pump beam, which comprises pulses of radiation, in response to radiation with laser driving beam 319. In order to provide efficient lasing, it is desirable to continually reflect the pump beam 307 onto Ti:Sapphire crystal 317. Therefore, the lasing crystal 317 is typically provided within a lasing cavity.

The driving beam 319 is directed onto crystal 317 using mirrors M1 and M2. The driving beam 319 can pass through mirror M3 and onto lasing crystal 317. The driving beam 319 which is not absorbed by crystal 317, is emitted through mirror M4. Mirror M4 serves to reflect any radiation back onto the lasing crystal 317. This radiation is then reflected via mirror M3 onto mirror M5 and onto output coupler 321. Output coupler 321 serves to reflect the pump beam 307 onto the frequency conversion member 315 to produce Terahertz radiation. The pump beam is focused onto frequency conversion member 315 via lens L1. Any radiation which is transmitted through the frequency conversion member 315 is reflected back through the frequency conversion member 315 by mirror M6. This radiation then impinges on output coupler 321.

Output coupler 321 transmits terahertz radiation, but it reflects most of the pump beam back onto mirror M5, which in turn reflects the radiation back onto the lasing crystal 317 via mirror M3. In other words, the lasing crystal 317 and the frequency conversion member 315 are all located within the same lasing cavity defined by mirror M6, the output coupler and mirrors M5, M3 and M4. The pump beam 307 is continuously reflected within this cavity to efficiently generate the pump beam and the THz beam.

The THz beam 53 which is emitted from output coupler 321 is directed into the imaging section 33 and onto sample 41 via THz imaging optics (not shown). The sample 41 is located on a motorised X-Y translation stage (not shown) so that the whole sample 41 can be imaged. (The x-y plane is orthogonal to the beam axis). The THz radiation carrying the imaging information from the sample is reflected into the THz detection system 35 via THz imaging optics 45.

Output coupler 321 transmits some visible radiation 55 as well as THz radiation as a reference beam 55. Imaging and electro-optic detection can be performed inside a single nitrogen-purged unit.

The sample 41 is mounted on a X-Y motorised translation stage (not shown) which is controlled by a PC computer (not shown). Each section (pixel) of the object may then be imaged. To improve the spatial resolution of the technique, off-axis parabolic mirrors, condenser cones, and lenses may be used to focus the beam to a diffraction limit spot. By mounting the sample in the near field of a condenser cone, the diffraction limit may be overcome and spatial resolution of about 50 μm may be achieved. The imaging system can function with or without such objects depending on the nature of the object to be imaged and the nature of the detection circuit.

Figure 3 shows the detection system in detail. The THz beam 39 carrying the imaging information and a visible light beam 55 are inputted into the THz detection system. The visible light beam 55 acts as a reference beam which is incident on the detection crystal 73. The reference beam 55 is linearly polarised and the polarisation is orientated such that it has components along both the ordinary and extraordinary axis of the detection crystal 73. Each of the axes has distinct refractive indices n_o and n_e along the ordinary and extraordinary axis of the crystal 73 respectively. In the absence of a second (THz) radiation beam 39, the linearly polarised reference beam 55 passes through the detection crystal 73 with negligible change in its polarisation.

The applicant wishes to clarify that the angle Θ through which the polarisation is rotated by is negligible. However, the linearly polarised beam can become slightly elliptical. This effect is compensated for by a variable retardation waveplate, e.g. a quarter waveplate 81.

The emitted beam 77 is converted into a circularly polarised beam 83 using quarter wave plate 81. This is then split into two linearly polarised beams by a Wollaston Prism 79 (or equivalent device for separating orthogonal polarisation components) which directs the two orthogonal components of the polarised beam onto a balanced photodiode 85. The balanced photodiode signal is adjusted using wave plate 81 such that the difference in outputs between the two diodes is zero.

However, if the detector 73 also detects a secondary beam 69 (in this case a beam with a frequency in the THz range) as well as a reference beam, the angle Θ through which the polarisation is rotated by is not negligible. This is because the THz electric field modifies the refractive index of the visible (fundamental) radiation along one of the axes n_e, n_o. This results in the visible field after the detector 73 being elliptical and hence the polarisation components separated by the prism 79 are not equal. The difference in the voltage between the output diodes gives a detection voltage.

The reference beam 55 and the THz beam 39 should stay in phase as they pass through the crystal 73. Otherwise the polarisation rotation Θ is obscured. Therefore, the detection crystal 73 has phase matching means to produce a clear signal.

Other types of generator may also be used. Figure 4 illustrates a so-called photoconductive emitter. The emitter comprises a member 91 comprising a semiconductor such as low temperature GaAs, GaAs, Si on Sapphire etc. The semiconductor member has a pair of electrodes 93a and 93b located on its surface. The electrodes 93a and 93b are connected to a power supply such that a field can be generated between the two electrodes 93a and 93b.

The simplest electrode arrangement is show in figure 4. However, the electrodes may be triangular and arranged in a bow-tie shape, a so-called bow-tie antenna or they may be interdigitated electrodes at the centre of a bow tie or spiral antenna. Alternatively, such designs may be incorporated into transmission lines on the chip.

The semiconductor member is irradiated by a pump beam which is a pulse of radiation (about 70fs) of the type which can be emitted by laser 37. The pulse comprises at least two frequencies ω_1 and ω_2, the difference of which gives a frequency in the THz regime. The pump beam impinges on the semiconductor member 91 on the part of its surface between the electrodes 93a and 93b, i.e. where the field is applied. The beating of the two visible or near-infrared frequencies in the non-linear region of the semiconductor member between the two electrodes 93a and 93b results in the emission of THz radiation from the semiconductor member 91. The semiconductor member 23 is provided with a lens 95, which may be of a hemispherical or other design, on its surface which is opposite to that of the surface with the electrodes, to allow the emission of a beam of THz radiation.

Figure 5 shows a further example of a detector which may be used with the imaging system of Figure 1. This type of detector is known as a photoconductive detector and comprises a detection member which may be, for example, GaAs, Si on Sapphire etc. The THz radiation is incident on the back surface of the detection member 96. The radiation is collected by lens 98 which may be hemispherical or have another shape. On the opposing side of the detection member 96 is located a pair of electrodes 97a and 97b. The region between these two electrodes 97a and 97b is illuminated by radiation of the visible or near infrared range.

The near-infrared/visible radiation illuminates the surface of the detector between the electrodes 97a and 97b. The Terahertz radiation which is collected by lens 98 induces a photocurrent through the region between the electrodes 97a and 97b which is being illuminated by the visible/infrared radiation. The current which can be detected by the electrodes is proportional to the strength of the THz field.

The electrode 97a, 97b may be of a simple diode formation embedded in a transmission line. Alternatively, they may be triangular and arranged in the shape of a bow-tie to from a so-called bow-tie antenna. They may also be interdigitated electrodes at the centre of a bow-tie or spiral antenna.

Figure 6 shows a schematic trace of a THz pulse which has been reflected from the sample using the type of apparatus which is shown for the example in Figure 1.

An oscillating electric field is plotted on the y axis against time along the x-axis. Typically, methods of extracting information from the trace have used either the position in time of the maxima of the electric field (T_1) or the position in time of the minima of the electric field (T_2).

As it can be seen from Figure 6, the magnitude of the measured electric field changes considerably with time. There is only a small time difference between T_1 and T_2. When looking at an area of the sample, a trace like the one shown in Figure 6 will be obtained for each point of the sample. The trace will change from point to point or pixel to pixel dependent on the composition of the sample.

Figure 7 shows a reflection image of a skin carcinoma. Figure 7a shows the THz image and Figure 7b shows the image using visible radiation.

To generate the image in Figure 7a, only reflected radiation from a single delay time i.e. a single point on the x axis of Figure 6, is plotted. The delay time may be the maxima of the electric field in some parts of the sample or the minima of the electric field in other parts of the sample. It can be seen that this image shows good contrast. As it is only necessary to measure the THz signal at a particular delay time, there is no need to continually sample the whole of the THz pulse. Therefore, the image can be produced using a much shorter acquisition time. Also, the image requires less processing.

Figures 8a and 8b show two images generated using THz radiation of a tooth. Figures 8a and 8b were produced in a similar manner to that of Figure 7. In other words, the image was taken for a single time delay. The time delay chosen was 0 picoseconds for Figure 8a.

Figure 8b shows the same tooth of Figure 8a, however, here the time delay is 6.99 picoseconds. It can be seen that the image in Figure 8b is far sharper than that of Figure 8a. The optimum image can be obtained by choosing the correct time delay.

Figure 9a shows a visible image of a tooth. The tooth is actually a slice through a tooth, the various regions such as the enamel-dentine region 201 and the pulp cavity region 203 can be distinguished. The enamel dentine region 201 has decayed due to caries in regions 205 and 207.

Figure 9b shows four THz traces plotted as amplitude of detected THz signal against time delay for three regions of the tooth and a reference signal. It can be seen that the reflected detected THz is quite different for the various regions. For example at peak 209, the signal taken in the enamel region (E) of the tooth is seen to dominate. Similarly, at peak 211, the dentine signal (D) is seen to dominate. At peak 213 the signal due to caries (C) dominates the trace. The reference signal (R) is generally seen to be the lowest peak.

By looking at the detected THz signals for different delay times, it is possible to distinguish differences between the different parts of the tooth.

Figures 9c, 9d and 9e show images of the tooth taken at times -0.08ps, 0.1ps and 3.34ps. These times correspond to the x axis of the Figure 9b. The trace as seen in Figure 9b will have to gathered for every part of the tooth of Figure 10a, but only for a single point on the x-axis, looking at a particular delay time is referred to as taking a time slice through the spectra.

The decayed regions 205 and 207 can be seen in all of figures 9c, 9d and 9e.

Figures 10a to 10d show further time slices of the tooth of figure 9a, which have not been optimised to illustrate carious regions 205 and 207. Comparing the time slices of Figures 10a to 10d with those of Figures 9c to 9e, it can be seen that the contrast especially in the caries region 205 and 207 is far more marked in Figures 9c to 9e as opposed to Figures 10a to 10b.

Figure 11 shows a range of different images for a tooth. The tooth used to generate the images of Figure 11 is different to the tooth used to generate the images of Figure 9. Here, a visible image of a slice through the tooth is shown in Figure 11a. It can be seen that there is no decay in this tooth. Figure 11b shows a THz absorption image of the tooth of Figure 11a. This is just simply obtained by measuring the electric field for each point on the tooth at the detector. The absorption image here is generated from all of the frequencies of the incident pulse of THz radiation, i.e. it is a panchromatic image.

Figure 11c is a so-called time of flight image. Returning momentarily back to Figure 9c which shows the THz trace, it can be seen that there is a maxima of the electric field. The time of flight image looks at this maxima and plots the change in temporal position of the this maxima for each point in the area of the sample being imaged.

As with the absorption and visible images, the pulp cavity 203 and the enamel dentine region 201 can be easily distinguished.

Figures 11d, 11e and 11f show time slices (similar to those described for Figures 9c to 9Ee) for delay times -0.1ps, 2.4ps and 3.1ps respectively. It can be seen that the contrast of the enamel dentine region 201 with the pulp cavity 203 changes dramatically between the three figures. Also, there is no indication of caries in any of the enamel regions in all of the time slices.

Figure 12 shows a further tooth. Figure 12a shows a visible image of the tooth, again the enamel dentine region 201 and the root/pulp cavity 203 can be easily determined. The tooth has a caries region 205 which can not be easily seen on the visible image 203. Figure 12b shows the absorption image which is obtained in the same way as Figure 11B.

Figure 12c shows a time slice. In both figures 12c and 12b, the caries region 205 can be easily seen. Figure 12d shows an image which is plotted by plotting the maxima of the electric field for each point of the sample which is irradiated. The enamel dentine region 201 can be seen. However, the caries region 205 is very weak and much weaker for that than the time slice shown in Figure 12c. The acquisition time for the time slice can be very fast because it is only necessary to detect the reflected THz for a single point in time.

Figure 13 shows a further image of a tooth. Figure 13a shows a visible image whereas Figure 13b shows a single plot of the THz reflected electric field against time. The THz image is taken along path 101 of the tooth. There are three strong features in the reflected THz. The first peak 103 is due to reflection of the THz from the enamel/air surface. The second peak 105 is due to reflection of the THz from the enamel/dentine interface e-d in the tooth. The third and weakest reflection is due to the dentine/pulp cavity interface d-p of the tooth.

Figure 14a shows a visible image of a slice of a tooth. The tooth has a healthy region 109 and a decayed region 111. Figure 14b shows a THz pulse in the time domain measured in the healthy region 109. Figure 14c shows a THz pulse measured in the time domain for the unhealthy region which is decayed due to caries 111. Returning to the visible image of the tooth slice in Figure 14a, two interfaces can be seen. The first is the enamel/air interface 113, the second is the enamel/dentine interface 115. In the THz trace, the healthy region two peaks 117 and 119 can be easily distinguished. The upper peak 117 is believed to be due to the reflection of the THz at interface 113, the second peak 119 is due to the reflection of THz at interface 115.

In the THz pulse of the unhealthy region, the peak due to the reflection from interface 113 is seen to be of almost the same height as the corresponding peak in Figure 14b. However, the second peak which is due to the reflection from interface 115 is seen to be much smaller. This is because a region of the tooth which is decayed due to caries absorbs THz far more strongly than a region which has not decayed. Hence, less of the THz penetrates as far as interface 115 and THz which is reflected from this interface is also more strongly absorbed than in the case of healthy teeth. Hence, peak 119 is considerably reduced in the trace of the unhealthy region.

Regardless of whether or not the tooth is healthy, the height of the peak from interface 113 should be identical in both traces b and c. However, due to their different positions on the tooth, possibly dirt on the surface of the tooth, they will almost always be different, therefore, in order to detect the presence of caries, the ratio of peak heights 117 and 119 between a healthy region and an unhealthy region should be compared.

This type of analysis does not only apply to teeth. Figure 15 shows a schematic of a healthy area of skin and an unhealthy area of skin. Figure 15b shows the THz pulse which has been reflected from a healthy region of the skin, Figure 15c shows a THz pulse in the time domain which has been reflected from an unhealthy portion of the skin.

In Figure 15a, a skin/air interface 121 is shown and a skin/fat interface 123. There is a healthy area 125 and an unhealthy area 127 which contains tumour 129. Figure 15b shows a THz time domain pulse for the healthy area 125. The first peak 131 is due to reflection from interface 121. The second peak 133 is due to reflection from skin/fat interface 123. Figure 15c shows a similar trace except here, it is taken in unhealthy region 127. The size of peak 131 remains virtually the same. However, the size of peak 133 is substantially reduced due to the absorption by the tumour 129.

By plotting the ratio of the reflection from the first interface 121 to the second interface 123, across the skin, the lateral extent of the tumour can be determined as shown in Figure 15d.

It is also possible to obtain information about the depth of a sample using reflection measurement which does not have particularly strongly defined interfaces. Lossy materials, such as biological samples have a relatively large absorption coefficient which dominates how radiation is reflected from the sample.

Figure 16, shows a THz pulse incident on a sample. The THz pulse propagates in the x-direction and is scattered (reflected) into a counter-propagating, or reflected, pulse by the object.

To simplify matters, the following analysis will only consider one spatial dimension (x) (i.e. for the case of a collimated THz beam path). It will also be assumed the object is uniform in the y-z plane over the dimensions of the THz beam. Given the 1-D analysis described here to provide information on the structure of the object in the x-direction, the variation of the object in the y-z directions may be obtained by scanning the object through the THz beam in the y-z plane (or, alternatively, scanning the THz beam over the object).

The analysis can be used to determine both how the absorption and the refractive index spatially varies within the sample. In practice, both the absorption coefficient and the refractive index vary also with frequency. The following analysis assumes that the frequency response of the refractive index is known and also that the absorption coefficient does not vary with frequency.

Since the electric field due to the reflected THz pulse may only be measured at discrete points in time, all the integral transforms below must be replaced by the appropriate discrete transform in order to operate on the finite dataset.

The incident and reflected THz pulses are characterised by electric fields $T(x,t)$ and $R(x,t)$ respectively. The quantities in brackets indicate that T and R are both functions of position, x, and time, t. It will be assumed that all electric fields are polarised along a similar axis perpendicular to the x-direction and hence they can be written as scalar quantities (i.e. ignore directional dependence):

$$T(x,t)= \int_{-\infty}^{\infty} T_\omega(x) \cdot e^{-i\omega t} \, d\omega$$

$$R(x,t)= \int_{-\infty}^{\infty} R_\omega(x) \cdot e^{-i\omega t} \, d\omega$$

where i is the imaginary unit $\sqrt{-1}$. The waves are written in their complex form; the true electric fields are obtained by taking the Real part of the complex waves. T_ω and R_ω are the complex amplitudes of the respective incident and reflected waves at each frequency component f where $f = \frac{2\pi}{\omega}$ and these quantities are also functions of position, x. The ω-subscripts indicate that a quantity is a function of ω. k is the wavevector of each frequency component of the wave and is defined by

$$k = \frac{n_\omega \omega}{c} + i \frac{\alpha_\omega}{2}$$

where c is the speed of light in a vacuum, n_ω and α_ω are the refractive index and absorption coefficients of the object at angular frequency ω. Thus both n_ω and α_ω may be functions of position and frequency. These are the materials parameters which characterise the object.

The propagation and coupling of energy between the incident and reflected waves is described by two, coupled 1st order differential equations (easily derived from Maxwell's Equations):

$$\frac{\partial T_\omega}{\partial x} + ikT_\omega = \frac{dk}{dx}\frac{1}{2k}R_\omega$$

$$\frac{\partial R_\omega}{\partial x} - ikR_\omega = \frac{dk}{dx}\frac{1}{2k}T_\omega$$

... Eq. 1

The left-hand-sides of the above equations describe the propagation of the two counter-propagating waves. The right-hand-sides provide the 'coupling' terms which transfer energy from one beam to the other in the presence of a scattering potential. In this case, the scattering potential is provided by a spatially varying wave-vector, k. I.e. $\frac{dk}{dx}$ must be non-zero for photons to be transferred from the incident wave to the reflected wave and vice versa. Where $\frac{dk}{dx} = 0$, there is no coupling between the beams and the incident and reflected waves propagate independently.

In a lossy, dispersive medium $\alpha{\neq}0$ and where n_ω is frequency dependent.

It will be assumed that the scattering potential is provided by a spatially varying coefficient, $\Delta(x)$ such that

$$k = k'\Delta$$

$$\frac{1}{k}\frac{dk}{dx} = \frac{d\Delta}{dx}$$

where k' is the spatial average of k and k' is independent of x. (k' remains a function of ω, while Δ is independent of ω).

In order to derive spatial information (i.e. information on how Δ varies with respect to x), it is necessary to know the spectral characteristics of the material in advance (i.e. to know how n_ω depends on ω). A functional form of $n_\omega(\omega)$ and also the coefficient α are

assumed. For the purposes of imaging, this may be calculated from the spatial average THz reflectivity of the sample (i.e. such that structural information is averaged out). The derivation of the *spectral* characteristics of a sample by THz reflection has been described elsewhere in the literature and will not be reproduced here.

For a lossy medium where $\alpha/_2 \gg n\omega/_c$ (such as water-based biological media) a Real spatial variation in Δ is due to a spatial variation in the absorption coefficient of the medium. Previously, only a spatial variation in the refractive index have been considered.

Furthermore, it is assumed that the spatial variation of k is much smaller than the absolute value of k i.e. $\dfrac{dk}{dx} \ll k$, and that the loss of energy from the incident wave due to reflection is much smaller than the loss due to absorption. These conditions are appropriate to most biological samples or sample of high water content. In this approximation, the spatial dependence of the incident wave is independent of the spatial variation of k and is given by

$$T_\omega(x) = T_{x=0 \atop \omega} e^{-ik'x}$$

where $T_{x=0}$ is the amplitude of the incident electric field at position x=0 and is a function of ω.

The spatial dependence of the reflected wave may now be described by a single differential equation:

$$\frac{dR_\omega}{dx} - ik'R_\omega = \frac{1}{2}\frac{d\Delta}{dx}T_{x=0 \atop \omega}e^{-ik'x} = \left(\frac{1}{2}\frac{d\Delta}{dx}T_{x=0 \atop \omega}.e^{-\frac{\alpha}{2}x}\right)e^{-i\frac{n_\omega\omega}{c}x}$$

$$= T_{x=0 \atop \omega}F(x)e^{-i\frac{n_\omega\omega}{c}x}$$

... Eq. 2

with $F(x) = \dfrac{1}{2}\dfrac{d\Delta}{dx}e^{-\frac{\alpha}{2}x}$

Equation 2 may be solved (by the method of Laplace transformation, for example), to obtain R_ω:

$$R_\omega(x) = T_{x=0 \atop \omega} \int_{x'=0}^{\infty} F(x')e^{i\frac{n_\omega \omega}{c}(x-2x')}dx'$$

Since it is necessary to measure the reflected wave at one point, we set x=0 to get

$$R_{x=0 \atop \omega} = T_{x=0 \atop \omega} \int_{x'=0}^{\infty} F(x')e^{-i\frac{n_\omega \omega}{c}2x'}dx' \qquad\qquad ..Eq.\ 3$$

This expression may be inverted to obtain *F(x)* under the assumption that *F* is independent of $\left(\dfrac{n_\omega \omega}{c}\right)$. This is not strictly true for systems where the absorption is a function of frequency. By making this assumption the analysis is simplified; the effect of the finite frequency dependence of the absorption coefficient is primarily to limit the spatial resolution (in the x-direction) of the final result, at frequencies where the frequency dependence is significant.

By inverse Fourier transformation of Equation 3 we get

$$F(x) = \frac{1}{2}\frac{d\Delta}{dx}e^{-\frac{\alpha}{2}x} \approx \frac{1}{2\pi}\int_{-\infty}^{\infty}\frac{R_{x=0 \atop \omega}}{T_{x=0 \atop \omega}}e^{i\frac{2n_\omega \omega}{c}x}d\left(\frac{2n_\omega \omega}{c}\right) \qquad\qquad ...\ Eq.\ 4$$

The spatial dependence of the parameter $\Delta(x)$ contains the structural information about the object which we are trying to deduce. This is obtained by rearranging Equation 4 and integrating over the position, x.

$$\Delta(x) = \frac{1}{2\pi} \int_{x=0}^{\infty} 2e^{\frac{\alpha}{2}x} \int_{\omega=-\infty}^{\infty} \frac{R_{x=0}}{T_{x=0}} e^{i\frac{2n_\omega \omega}{c}} \left(\frac{2n_\omega}{c} + \frac{2\omega}{c} \frac{dn_\omega}{d\omega} \right) d\omega\, dx \qquad \ldots Eq.\ 5$$

The factor $R_{x=0,\ \omega}$ is obtained by Fourier transform of the measured reflected THz electric field, $R(t)$ (i.e. as measured at point x=0, corresponding to the surface of the medium or sample):

$$R_{x=0 \atop \omega} = \frac{1}{2\pi} \int_{t=0}^{\infty} R(t) e^{i\omega t}\, dt$$

The factor $T_{x=0,\ \omega}$ is obtained by Fourier transform of a reference THz pulse. The THz reference pulse may be obtained by measuring the THz pulse reflected off a sample of known reflectivity such as a silver mirror, for example. The THz pulse reflected from a silver mirror is an exact replica of the incident THz pulse i.e.

$$T^{silver}(t) = R^{silver}(t)$$

A similar transformation is performed on $T(t)$:

$$T_{x=0 \atop \omega} = \frac{1}{2\pi} \int_{t=0}^{\infty} T(t) e^{i\omega t}\, dt$$

In practice, the incident THz pulse must have a finite bandwidth; that is, $T_{x=0,\ \omega}$ will drop below the noise-level of the measurement apparatus at frequencies above some threshold, ω_{max}. Similarly, $T_{x=0,\ \omega}$ will drop below the measurement noise at frequencies below some minimum threshold, ω_{min}. In order to exclude artefacts due to noise where $T_{x=0,\ \omega}$ has become small, we included a windowing function $W(\omega)$. This function has the property that it drops to zero at both high and low frequencies faster than $T_{x=0,\ \omega}$.

For example, we may choose $W_\omega = W(\omega)$ to be a square-pulse function:

$$\begin{cases} W(\omega) = 1; & \omega_{min} < \omega < \omega_{max} \\ W(\omega) = 0; & \text{all other } \omega \end{cases}$$

The final result is

$$\Delta(x) = \frac{1}{2\pi} \int_{x=0}^{\infty} 2e^{\frac{\alpha}{2}x} \int_{\omega=-\infty}^{\infty} \frac{R_{x=0}}{T_{x=0}} W_\omega e^{i\frac{2n_\omega\omega}{c}} \left(\frac{2n_\omega}{c} + \frac{2\omega}{c} \frac{dn_\omega}{d\omega} \right) d\omega \, dx \qquad \dots \text{Eq. 6}$$

$\frac{dn_\omega}{d\omega}$ may be calculated directly from the previously determined functional form of n_ω.

Equation 6 constitutes the main result. $\Delta(x)$ is obtained by numerical evaluation of Equation 6, once all the constituent factors have been determined. Since Δ is complex either the real or the imaginary part of the function may be plotted to form an image, or some combination. Δ obtained in this way is considered only an approximation to the exact structural form of the sample, in view of the approximations described above.

CLAIMS:

1. A method of investigating a sample, the method comprising the steps of:
    irradiating a surface of a sample with a pulse of electromagnetic radiation, said pulse having a plurality of frequencies in the range from 25 GHz to 100 THz;
    detecting said radiation reflected from the sample and deriving structural information about the sample as a function of depth from the surface of the sample.

2. A method according to claim 1, wherein the sample comprises biological material.

3. A method according to claim 1, wherein the step of deriving structural information about the sample, comprises the step of deriving the absorption or refractive index as a continuous function of depth.

4. A method according to any preceding claim, the method further comprising the step of detecting a reference signal.

5. A method according to claim 4, wherein the reference signal is detected by reflecting radiation from a mirror which is substantially perfectly reflecting.

6. An apparatus for investigating a sample, the apparatus comprising:
    means for irradiating a surface of a sample with pulse of electromagnetic radiation, said pulse having a plurality of frequencies in the range from 25 GHz to 100 THz;
    means for detecting said radiation reflected from the sample and deriving structural information about the sample as a function of depth from the surface of the sample. means

7. A method of imaging a sample, the method comprising the steps of:

irradiating a sample with a pulse of electromagnetic radiation, said pulse having a plurality of frequencies in the range from 25 GHz to 100 THz;

detecting the amplitude of the radiation reflected from or transmitted by the sample; and

generating an image of sample using the amplitude of the radiation detected at a single point in time.

8.   A method according to claim 7, wherein the amplitude of the radiation is detected for a period of time, and the image is generated for a single time point.

9.   A method according to claim 8, wherein the step of generating the image comprises the step of generating a plurality of images for a plurality of different time points.

10.   A method according to claim 9, further comprising the step of optimising the contrast of the image generated using time points as an optimising parameter.

11.   A method according to claim 7, wherein the radiation is only detected for a single time point.

12.   An apparatus for generating an image of a sample, the apparatus comprising:
means for irradiating a sample with a pulse of electromagnetic radiation, said pulse having a plurality of frequencies in the range from 25 GHz to 100 THz;

means for detecting the amplitude of the radiation reflected from or transmitted by the sample; and

means for generating an image of sample using the amplitude of the radiation detected at a single point in time.

13.   An apparatus according to claim 12, the apparatus further comprising means for displaying a plurality of images generated from different time points.

28

14.   A method of detecting variation in the composition of a sample, the variations being located between a first and second interfaces of the sample, the method comprising the steps of:

irradiating a first part and a second part of a surface of the sample with electromagnetic radiation, the first interface being located closer to the surface than the second interface;

detecting the signal due to reflection of the radiation from the first and second interfaces of the two parts of the sample;

comparing the peak height of the signal from the second interface with that of the first interface in the same part of the sample to produce a corrected second interface signal and comparing the corrected second interface signals.

15.   A method according to claim 14, wherein the sample is a tooth and the first and second interfaces are chosen from the external surface of the tooth, the enamel/dentine interface of the pulp cavity/dentine interface.

16.   A method according to claim 14, wherein the sample is a human or animal body part and the first and second interfaces are chosen from the outer layer or the skin, the skin/fat interface, or an interface within the skin.

17.   A method according to any of claims 14 to 17, further comprising the step of deriving the connected second interface signal for a plurality of parts.

18.   A method according to claim 17, wherein the method further comprises the step of generating a plot or image by plotting the connected second signal for a plurality of adjoining parts of the sample.

19.   An apparatus for detecting variation in the composition of a sample, the variations being located between a first and second interfaces of the sample, the apparatus comprising:

means for irradiating a first part and a second part of a surface of the sample with electromagnetic radiation, the first interface being located closer to the surface than the second interface;

means for detecting the signal due to reflection of the radiation from the first and second interfaces of the two parts of the sample;

means for comparing the peak height of the signal from the second interface with that of the first interface in the same part of the sample to produce a corrected second interface signal and comparing the corrected second interface signals for the different parts of the sample.

20. A method as substantially hereinbefore described with reference to the accompanying drawings.

21. An apparatus as substantially hereinbefore described with reference to any of the accompanying figures.

Application No: GB 0005225.8   **Examiner:** Eamonn Quirk
Claims searched: 1-13   **Date of search:** 22 April 2000

Patents Act 1977
Search Report under Section 17

Databases searched:

UK Patent Office collections, including GB, EP, WO & US patent specifications, in:

   UK Cl (Ed.R): G1A(AAMA, AAMX,) H5R(RAT, RTQ, RAD)

   Int Cl (Ed.7): G01N(21/35, 21/47, 21/49, 21/84) A61B(5/00, 6/14)

Other: Online: WPI, JAPIO, EPODOC

Documents considered to be relevant:

Category	Identity of document and relevant passage		Relevant to claims
X	EP 0 864 857 A1	(Lucent Technologies)Whole Document	1-3,6-9, 11-13
A	EP 0 828 143 A1	(Lucent Technologies)Whole Document	
A	EP 0 828 162 A2	(Lucent Technologies)Col.2 line 33- col.3 line 17.	
A	US 5 710 430	(Lucent Technologies) Col.2 lines 30-54	

X	Document indicating lack of novelty or inventive step	A	Document indicating technological background and/or state of the art.
Y	Document indicating lack of inventive step if combined with one or more other documents of same category.	P	Document published on or after the declared priority date but before the filing date of this invention.
&	Member of the same patent family	E	Patent document published on or after, but with priority date earlier than, the filing date of this application.